International Journal of Bifurcation and Chaos, Vol. 19, No. 8 (2009) 2717–2726

NONVARIATIONAL ISING–BLOCH TRANSITION IN PARAMETRICALLY DRIVEN SYSTEMS

MARCEL G. CLERC, SALIYA COULIBALY*
and DAVID LAROZE†
Departamento de Física,
Facultad de Ciencias Físicas y Matemáticas,
Universidad de Chile, Casilla 487-3, Santiago, Chile
**Laboratoire de Cristallographie et Physique Moléculaire (LACPM),*
UFR Sciences des Structures de la Matière et Technologies (UFR SSMT),
Université de Cocody, Abidjan, Côte d'Ivoire
†*Instituto de Alta de Investigación,*
Universidad de Tarapacá, Casilla 7D, Arica, Chile

Received April 3, 2008; Revised October 2, 2008

Transition from motionless to moving domain walls connecting two uniform oscillatory equivalent states in both a magnetic wire forced with a transversal oscillating magnetic field and a parametrically driven damped pendula chain are studied. These domain walls are not contained in the conventional approach to these systems — parametrically driven damped nonlinear Schrödinger equation. By adding in this model higher order terms, we are able to explain these solutions and the transition between resting and moving walls. Based on amended amplitude equation, we deduced a set of ordinary differential equations which describes the nonvariational Ising–Bloch transition in unified manner.

Keywords: Nonequilibrium systems; font propagation; localized structures.

1. Introduction

Nonequilibrium processes often lead in nature to the formation of spatially homogeneous states, oscillatory states, patterns, waves, spatio-temporal chaos state or localized structures with nontrivial dynamical behaviors, to mention a few. Different states frequently co-exist in the same region of parameters at variance with equilibrium systems [Nicolis & Prigogine, 1977]. The interaction of different states is characterized by fronts or domain walls or defects, which are interfaces between them [van Saarloos, 2003]. For example, bistable systems can exhibit fronts connecting two homogeneous states. The features and dynamics of such domain walls have attracted attention across many areas of science, including biology, chemistry and physics [Murray, 1989]. Generically, a front connecting two different uniform states moves in such a way that the more stable state invades the other [Residori *et al.*, 2004; Clerc *et al.*, 2004]. In the case of one- or two-dimensional gradient or variational systems and small interface curvature, the front velocity is proportional to the energy difference between the two states. This velocity can be modified by the curvature of the front, according to the Gibbs–Thomson effect [Burton *et al.*, 1951]. Changing parameters, the metastable state — less stable state — becomes energetically equivalent to the other state, thus the front stops propagating; in particular, the system is said to be at the Maxwell point [Goldstein *et al.*, 1991]. By further increment of the parameters, the

front speed is reversed, that is, the most energetically favored state invades the less favored one.

The afore-mentioned scenarios change drastically, when one considers a system with discrete symmetry — for instance the reflection symmetry — and when this system possesses two equivalent homogeneous states. The domain walls connecting such states are generically at rest as a consequence to the discrete symmetry. Both states are "energetically" equivalents. However, under spontaneous breaking of symmetry these fronts can hold nonzero asymptotic speed. A classical example of such phenomenon is the so-called Ising–Bloch Transition [Coullet *et al.*, 1990] observed in ferromagnets [Bulaevsky & Ginzburg, 1964], liquid crystal [Gilli *et al.*, 1994], and chemical reactions [Haim *et al.*, 1996]. Gradient or variational systems do not exhibit this phenomenon, since the front speed is proportional to energy difference between these equivalent states. The dynamics of a nongradient system can always be discomposed into two parts, a dissipative and a remnant; such that a Lyapunov functional — *Nonequilibrium potential* — characterizes the dissipative dynamics [Graham & Tel, 1986]. The steady states of nonequilibrium systems minimize the nonequilibrium potential and the remnant dynamics is responsible for nontrivial dynamics of stationary states like oscillations, chaos and so forth. Therefore, the front propagation in the nonequilibrium Ising–Bloch transition is a consequence of remnant dynamics [Barra *et al.*, 1996]. Due to the universal nature of walls propagation linking two equivalent uniform states, the transition between a resting to a moving front is usually denominated nonvariational or nonequilibrium Ising–Bloch transition [Michaelis *et al.*, 2001].

The aim of this article is to study the nonvariational Ising–Bloch transition between two uniform oscillatory equivalent state observed numerically in both a magnetic wire forced with a transversal oscillatory magnetic field and a parametrically driven damped pendula chain. These domain walls are not contained in the conventional approach to these systems — the parametrically driven damped nonlinear Schrödinger equation. Adding in this model the higher order terms, we are able to explain these states and the transition between resting and moving walls. Hence, using this *amended amplitude equations* we recover the original dynamical behavior of these systems. From the amended amplitude equation, we derive a set of ordinary differential equations which describe the nonvariational Ising–Bloch transition in unified manner.

The manuscript is organized as follows. In Sec. 2, the nonvariational Ising–Bloch transition in parametrically driven magnetic system and damped pendula chain is described. In Sec. 3 is proposed an amended amplitude equation, which describes in unified manner the nonvariational Ising–Bloch transition exhibited by parametrically driven systems. A simple differential ordinary equations is deduced in Sec. 4, to explain the Ising–Bloch transition. Finally, the conclusions are presented in Sec. 5

2. Moving Domain Walls in Parametrically Driven Systems

In this section, we expose our theoretical model of moving domain wall for two different quasi-reversible prototype systems: parametrically driven magnetic system and vertically driven pendula chain.

2.1. *Parametrically driven magnetic system*

A one-dimensional easy-plane ferromagnetic like $CcNiF_3$ or TMMC or $Ni_{80}Fe_{20}$ is described by the well-known Landau–Lifshitz–Gilbert equation, which in dimensionless form may be written as [Barashenkov *et al.*, 1991]

$$\begin{aligned}\partial_t \mathbf{M} = \mathbf{M}\times\mathbf{M}_{zz} - \beta(\mathbf{M}\cdot\hat{z})(\mathbf{M}\times\hat{z})\\ + \mathbf{M}\times\mathbf{H} - \alpha\mathbf{M}\times\mathbf{M}_t\end{aligned} \tag{1}$$

where $\mathbf{M}$ stands for the unit vector of the magnetization, $\beta > 0$ is the easy-plane anisotropy constant, $\hat{z} \equiv (0,0,1)$ denotes the unit vector along the hard axis, and α is the relaxation constant. Let us consider an external magnetic field $\mathbf{H} = (H_0 + h_0 \sin\omega t)\hat{x}$, which has both a constant and a periodic forcing with amplitude h_0 and fixed frequency ω. Figure 1 depicts the set up of the system under study.

A trivial state of Eq. (1) is the homogeneous magnetization $\mathbf{M} = \hat{x}$. When the magnetic wire is forced close to the double of the natural frequency $\omega = 2(\omega_0 + \nu)$ ($\omega_0 \equiv \sqrt{H_0(\beta + H_0)}$ in units of the gyro-frequency, where 2ν is the detuning parameter) the homogeneous magnetization becomes unstable at $h_0^2/4\omega_0^2 = \alpha^2 + 4\nu^2/(\beta + 2H_0)^2$ for small $\{\nu, h_0, \alpha\}$ — Arnold's tongue. This bifurcation gives rise to a uniform or synchronized precession motion of the magnetization around the

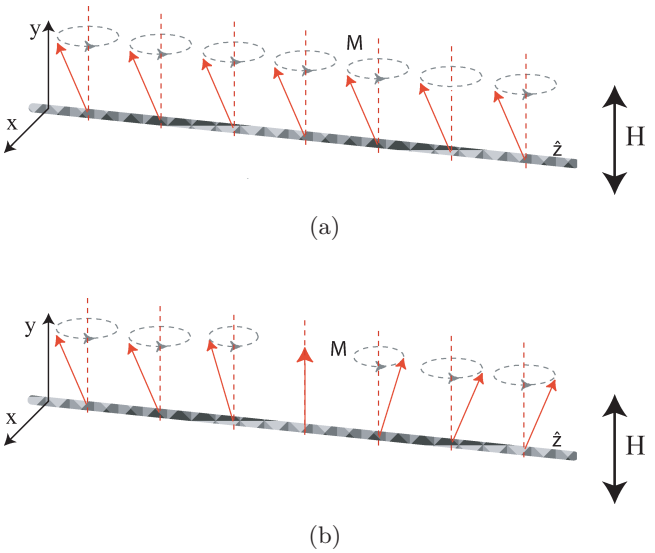

Fig. 1. Schematic representation of the parametrically driven magnetic wire and the different states exhibited by the set-up. (a) The homogeneous precession, and (b) the domain wall that links two uniform precessions.

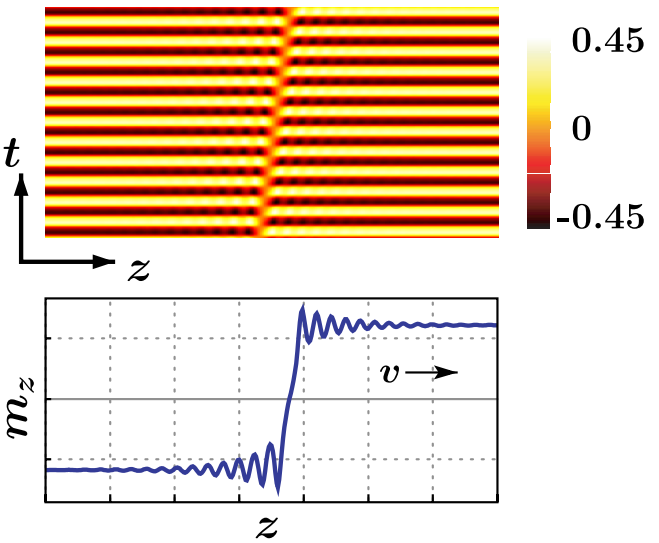

Fig. 3. Density plot of spatio-temporal diagram of M_z for Bloch type wall exhibited by Landau–Lifshitz–Gilbert Eq. (1) with $\beta = 6$, $H_0 = 1.125$, $h_0 = 0.775$, $\omega = 2(\sqrt{H_0(H_0+\beta)} + \nu)$, $\nu = -0.05$ and $\alpha = 0.09$.

easy axis $\hat{x}$ in the yz-plane with frequency ω_0 [Clerc *et al.*, 2008]. Figure 1(a) depicts the uniform precession for the corresponding magnetization field and Fig. 2(a) shows numerical simulation of these state for model (1). Due to the reflection symmetry $\mathbf{M} = (M_x, M_y, M_z) \to (M_x, -M_y, -M_z)$ of Eq. (1), there is another uniform precession solution out of phase in π. Hence, we can expect to find solutions

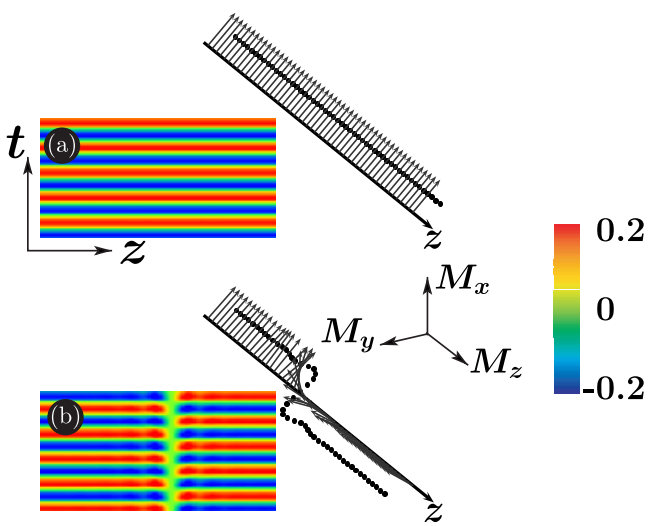

Fig. 2. Density plot of spatio-temporal diagram of the M_z component of magnetization obtained from the Landau–Lifshitz–Gilbert Eq. (1) inside Arnold's tongue for $\beta = 20$, $H_0 = 1$, $h_0 = 0.57$, $\omega = 2(\sqrt{H_0(H_0+\beta)} + \nu)$, $\nu = -0.057$ and $\alpha = 0.05$. (a) Homogeneous state, and (b) Kink state between two synchronized precessions shifted by π.

that link these two uniform precessions — kink or domain wall solutions. Figure 2(b) displays the typical domain wall for parametrically driven magnetic system and the components of the magnetic field obtained from the Landau–Lifshitz–Gilbert model (1). In a large region of parameters space, these domain walls are motionless — Ising type wall. However, a decrease in the detuning parameter, inside the Arnold's tongue, produces the motion of the interfaces — Bloch type wall. Depending on the initial condition, the interface propagates to the right or the left, because the initial condition breaks the spatial reflection symmetry ($x \to -x$). Further decreasing of the detuning increases the wall speed. Figure 3 illustrates the typical Bloch wall observed in model (1) and the characteristic spatio-temporal dynamics exhibited by this moving front. For a large negative detuning the uniform processions become unstable, then the moving interfaces become also unstable. It is important to note that the Ising and Bloch type walls are spatial symmetric and asymmetric solutions with respect to the wall core, respectively. Hence, Bloch type walls have well-defined chirality since the integration of $M_y(x,t)$ around wall core is not null at variance of the Ising type wall [Coullet *et al.*, 1990].

2.2. *Vertically driven pendula chain*

To emphasize the robust nature of nonvariational Ising–Bloch transition, we consider a parametrically

driven damped pendula chain, which is modeled in the continuum limit by

$$\ddot{\theta}(z,t) = -(\omega_o^2 + \gamma\sin(\omega t))\sin(\theta) - \mu\dot{\theta} + k\partial_{zz}\theta, \tag{2}$$

where $\theta(z,t)$ is the angle formed by the pendulum and the vertical axis in the z-position at time t; ω_o is the pendulums' natural frequency, and $\{\mu, k, \gamma, \omega\}$ are the damping, elastic coupling, amplitude and frequency of the parametric forcing, respectively.

A simple homogeneous state of Eq. (2) is $\theta = 0$, which represents a uniform vertical oscillation of pendula. When the pendula chain is forced close to the double of the natural frequency — $\omega = 2(\omega_0+\nu)$, where 2ν is the detuning parameter — the vertical solution becomes unstable at $\nu^2 + \mu^2/4 = \gamma^2/16$ for small $\{\nu, \gamma, \mu\}$ — Arnold's tongue. This bifurcation gives rise to a uniform attractive periodic solution, so the pendula chain oscillates uniformly ($\theta(t+T) = \theta(t)$ where $T \approx 2\pi/\omega_0$). Due to the reflection symmetry — $\theta \to -\theta$ — there is another uniform oscillation out of phase in π. Hence, we expect to find again a solution that connects these two spatially uniform oscillations: kink or wall solutions. Figure 4 depicts the domain wall solution exhibited by the model (2). Similar dynamics behavior to those exhibited by the domain walls in parametrically driven magnetic wire is now observed in parametrically driven damped pendula chain. That means, inside of first Arnold's tongue and large detuning, domain walls are motionless; next, decreasing the detuning the Ising type walls become unstable and give rise to moving interfaces with a well-defined speed. The interface speed increases when the detuning decreases.

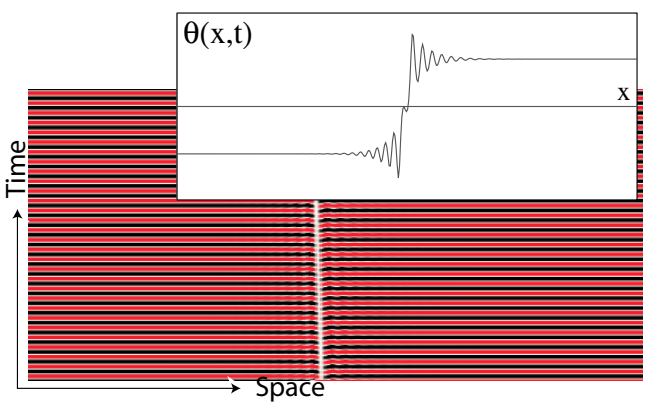

Fig. 4. Density plot of spatio-temporal dynamics of $\theta(x,t)$ for Bloch type wall exhibited by parametrically driven damped pendula chain Eq. (2), with $\omega_0 = 1.0$, $\omega = 2(\omega_0+\nu)$, $\nu = -0.06$, and $\mu = 0.2$. Inset picture is an instantaneous profile of the field $\theta(x,t)$.

In brief, parametrically driven systems such as magnetic or mechanic can exhibit a nonvariational Ising–Bloch transition. In the next section, we present a unified treatment of this phenomenon.

3. Unified Description of Parametrically Driven Instability

To account for the dynamics exhibited by both previous systems, we consider the time reversal limit perturbed with small injection and dissipation of energy: the quasi-reversal limit [Clerc *et al.*, 1999a, 1999b, 2001]. In this limit the dynamics of our prototype systems can be described by the parametrically driven damped nonlinear Schrödinger equation:

$$\partial_\tau A = -i\nu A - i|A|^2A - i\partial_x^2 A - \mu A + \gamma\overline{A}, \tag{3}$$

where A is the envelope of the uniform oscillation, and $\{\nu, \mu, \gamma\}$ stand for the detuning between the natural and the twice forcing frequencies, the damping and the forcing, respectively. For example, the quasi-reversal limit of model (2) is described by the perturbed Sine–Gordon equation with $\gamma \sim \nu \sim \mu \sim \epsilon$, where ϵ is an arbitrary small scale $\epsilon \ll 1$. Considering the following ansatz

$$\theta(z,t) = 2\sqrt{\frac{\varepsilon}{\omega_o}}A(\tau,x)e^{i(\omega_o+\nu)t} - 2\sqrt{\frac{\varepsilon}{\omega_o}}\left\{\frac{A^3(\tau,x)}{48} + \frac{i\gamma}{16\omega_0^2}A(\tau,x) - \frac{i\gamma\varepsilon}{8\omega_0^3}|A(\tau,x)|^2A(\tau,x)\right\} \times e^{3i(\omega_o+\nu)t} + c.c + \text{h.o.t}, \tag{4}$$

where $\tau = \varepsilon t$, $x = \sqrt{2\varepsilon\omega_0/k}z$ are slow variables, in Eq. (2); after straight-forward calculation the amplitude A satisfies Eq. (3). The explicit terms of the above equation are of order $\varepsilon^{3/2}$ and h.o.t. are at least of order $\varepsilon^{5/2}$. In a similar manner, we can deduce the amplitude equation (3) from model (1). This model has been used intensively to describe patterns and solitons in several systems such as: vertically oscillating layer of water [Zhang & Viñal, 1995], localized structures in nonlinear lattices [Denardo *et al.*, 1992], and the Kerr type optical parametric oscillator [Longhi, 1996], to mention a few.

The parametrically driven damped nonlinear Schrödinger equation has the homogeneous state, $A = 0$, which represents $\theta(x,t) = 0$ and

$M(x,t) = \hat{x}$, respectively. Inside the Arnold's tongue this model also has the uniform states

$$A_{\pm} = \pm\left(1 + i\sqrt{\frac{\mu-\gamma}{\mu+\gamma}}\right)x_0,$$

where $x_0 \equiv \sqrt{(\gamma-\mu)(-\nu+\sqrt{\gamma^2-\nu^2})/2\gamma}$. These three states merge together through a pitchfork bifurcation at $\gamma^2 = \mu^2+\nu^2$, with $\nu > 0$. The $|A_{\pm}|$ represents, respectively, the amplitude of the homogeneous oscillations for the pendula chain and the magnetic forced wire. However, these uniform states are linear unstable fixed points for the parametrically driven damped nonlinear Schrödinger equation. Also, they are marginal for $\nu = 0$, that is, whatever perturbations of the form $A = A_{\pm} + a_0 e^{\lambda t+ik}$ ($a_0 \ll 1$) satisfy $\lambda(k) \leq 0$ and there are critical wave numbers $k_c = \pm\sqrt{-\nu+2\sqrt{\gamma^2-\mu^2}}$ for which $\lambda(k_c) = 0$. At this surface in the parameters space ($\nu = 0$), we observe numerically that the uniform state is nonlinearly stable; however, kink states which connect these states are unstable. Hence, the model (3) does not account for features of homogenous oscillation and consequently it is unable to describe domain walls observed in the original systems. Since all these solutions asymptotically converge to the uniform states, the stability of these particle type solutions depend on the steadiness of these uniform states.

To describe the domains walls exhibited by the pendula chain and the magnetic forced wire under study, it is required to consider higher order terms in the amplitude equation (3), since the addition of these terms may restore the features of the uniform states and the particle type solutions. In the parameters region where the uniform state $|A_{\pm}|$ is marginal ($\nu = 0$), we expect that any small corrections of the amplitude equation can render this state linear stable or unstable. Consequently, when we consider the higher order terms the amplitude equation reads:

$$\begin{aligned}\partial_t A = &-i\mu A - iA|A|^2 - \partial_x^2 A - \nu A + \gamma\overline{A} \\ &+ ib|A|^4 A - \delta|A|^2\overline{A} + \alpha A^3. \end{aligned} \quad (5)$$

Let us denominate Eq. (5) as *Amended amplitude equation*, where $\{\delta, \alpha\}$ account for nonlinear forcing terms, which are proportional to the amplitude of the forcing and b stands for the nonlinear response in frequency and this parameter is order one. For example, in the parametrically driven damped pendula chain these parameters are

$$b \equiv \frac{1}{6\omega_0}, \quad \delta \equiv \frac{3\gamma}{8\omega^2}, \quad \text{and} \quad \alpha \equiv \frac{7\gamma}{24\omega^2}.$$

The extra terms in Eq. (5) are order $\varepsilon^{5/2}$ and the dominating terms are of order $\varepsilon^{3/2}$. For small detuning, we observe numerically that the amended amplitude equation (5) has stable uniform solutions close to A_+ or A_-, and in this parameters region Eq. (5) exhibits stable solutions connecting these states — kink or Ising type solutions.

Figure 5 shows these wall type solutions. Numerically, we observe that inside the Arnold's

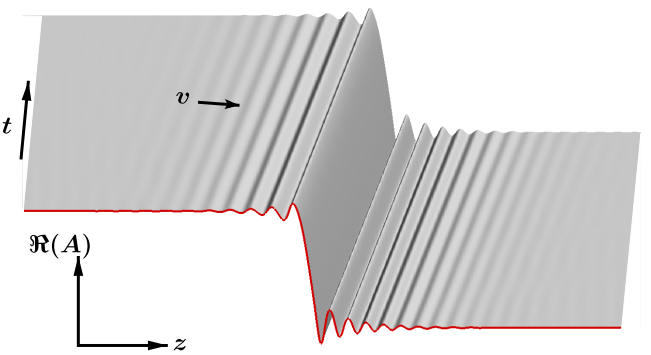

Fig. 5. Spatio-temporal diagram of Bloch type solution exhibited by model (5) with $\gamma = 0.8$, $\mu = 0.2$, $\nu = -0.07$, $b = 0.167$, $\delta = 0.3$ and $\alpha = 0.233$.

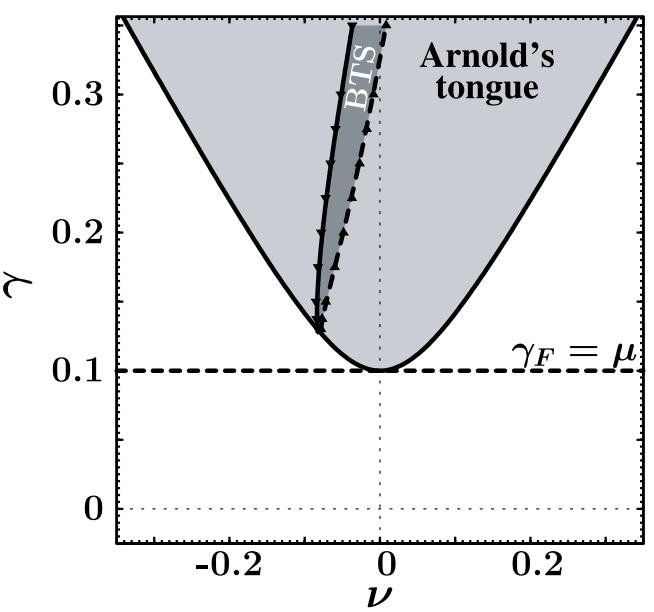

Fig. 6. Bifurcation diagram of amended amplitude equation (5). The gray and dark gray areas stand for the Arnold's tongue and the region of moving walls or Bloch type solution (BTS). The dashed and continuous lines Arnold's tongue represent the nonvariational Ising–Bloch transition and the spatial instability of the uniform non-null states.

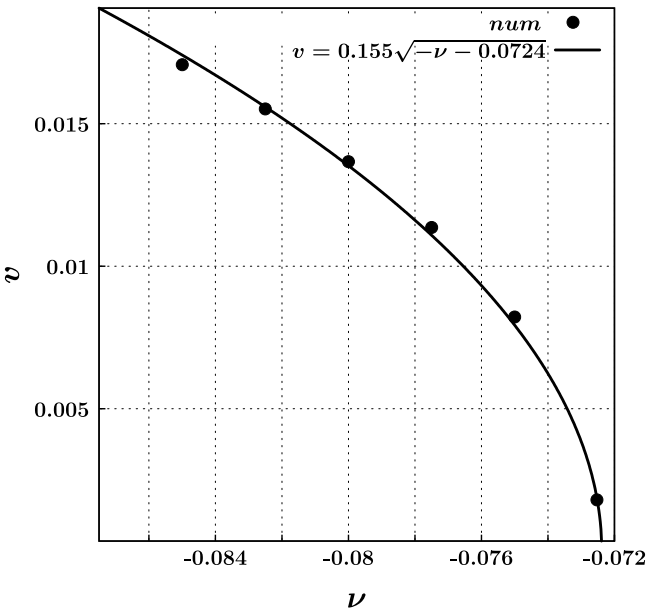

Fig. 7. Velocity of Bloch type wall as a function of detuning for amended amplitude equation (5). The dot points are the numerical wall speed obtained by $\gamma = 0.6$, $\mu = 0.2$, $b = 0.167$, $\delta = 0.225$ and $\alpha = 0.175$. The continuous curve is obtained using the square root law.

tongue the Ising type walls are motionless for positive detuning and small forcing. Nevertheless, for negative detuning in a large region of parameters inside Arnolds tongue, these interfaces become a moving wall (see Fig. 6). Decreasing the detuning, the wall speed increases as square root law of detuning minus a critical value of it. Figure 7 depicts the wall speed as a function of the detuning. The dashed line in Fig. 6 accounts for the transition between motionless to moving interface, nonvariational Ising–Bloch transition. This dashed curve has been computed numerically by determining the origin of square root law for wall speed.

4. Wall Speed Model

To understand the mechanism of the nonequilibrium Ising–Bloch transition, we compute the spectrum — set of eigenvalues — of the linear operator (which is denominated $\mathcal{L}(x)$) that describes the dynamics of small perturbation around the Ising type wall close to the transition. The lack of an analytical expression for the Ising type wall only allows us to compute numerically the spectrum, and their respective eigenfunctions.

The typical spectrum observed near and below the transition is shown in Fig. 8. Due to the translation invariance symmetry, $x \to x + x_0$, the spectrum always has an eigenvalue at the origin of complex plane and its respective eigenfunction is denominated as Goldstone mode. Inset figure in Fig. 8 depicts this mode. This mode characterizes the fact

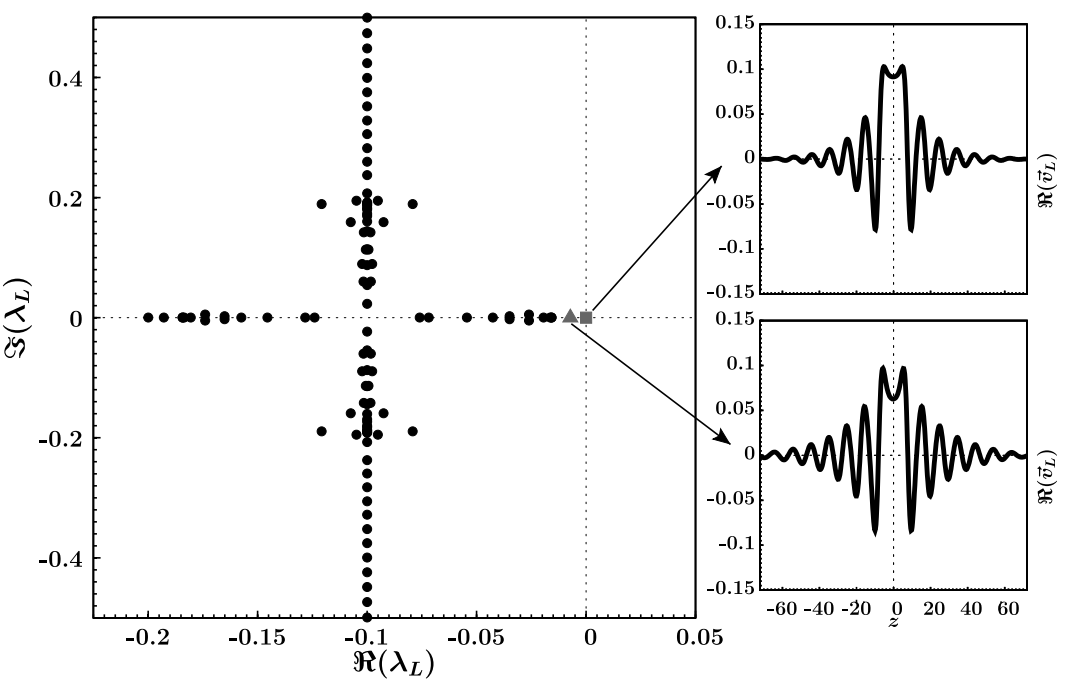

Fig. 8. Spectrum of linear operator which characterizes the linear stability of the Ising type wall of the model (5) with $\gamma = 0.6$, $\mu = 0.2$, $\nu = -0.06$, $b = 0.167$, $\delta = 0.225$ and $\alpha = 0.175$. Inset figures are the real part of the eigenfunctions of the respective critical modes.

that an infinitesimal spatial translation of the Ising type wall is also a solution. When the parameters are changed further more close to transition, then there is an eigenvalue with zero imaginary and real negative part which move to the origin of complex space. This eigenvalue and its respective eigenfunction are depicted in Fig. 8 by a triangle and the lower inset picture. Note that this eigenfunction is an asymmetrical function with respect to the spatial center — core of the kink. At the transition, this eigenvalue collides with the eigenvalue related to Goldstone mode at the origin of complex plane.

Subsequently, the mechanism of the Ising–Bloch transition is that an asymmetrical spatial mode becomes unstable, namely, the system exhibits a spontaneous breaking of symmetry [Coullet *et al.*, 1990]. This transition is characterized by two critical modes, the asymmetrical and the symmetric Goldstone modes, where these modes are related to the chirality and wall speed. To describe the wall dynamic close to the transition of model (5), we use the following ansatz

$$A(x,t) = |A_{\text{Ising}}(x - P(\varepsilon t))\rangle + \varepsilon\chi(\varepsilon t)|A_{as}(x-P)\rangle + |W(x,P,\chi)\rangle, \tag{6}$$

where $|A_{\text{Ising}}(x-P)\rangle$ is the Ising type solution, which is known only numerically, P stands for the position of the core of the Ising type wall, that is $|A_{\text{Ising}}(0)\rangle = 0$, $|A_{as}(x-P)\rangle$ is the critical mode of the square of the linear operator $\mathcal{L}$, which is obtained using the standard Jordan construction ($\mathcal{L}^2|A_{as}\rangle = 0$ and $\mathcal{L}|A_{as}\rangle = |\partial_z A_{\text{Ising}}\rangle$), $\chi(t)$ accounts for the amplitude of asymmetrical part (chirality), $|W\rangle$ is a small complex correction function ($|W| \ll 1$) whose temporal dependence is implicit through the variable $\{P,\chi\}$ and ε is an arbitrary small scale ($\varepsilon \ll 1$) which is square order of bifurcation parameter of the transition. Figure 9 shows the two eigenfunctions of the operator $\mathcal{L}^2$, the lower inset picture is $|A_{as}\rangle$, confirming the Jordan construction.

Notice that the above ansatz is based on the standard parameter variation method. Replacing the above ansatz in the amended amplitude equation (5) and linearized in $|W\rangle$ formally one obtains

$$-\varepsilon\dot{P}|\partial_z A_{\text{Ising}}(z)\rangle + \varepsilon^2\dot{\chi}|A_{as}(z)\rangle = \mathcal{L}|W\rangle + H(\chi,z,\varepsilon), \tag{7}$$

where $z \equiv x - P(t)$ is an auxiliary variable, the upper dot means temporal derivative and H is a complex function. As result of spatial reflection symmetry ($z \to -z$) and spatial invariance the function H is an odd function of chirality and is independent of P, this implies that

$$H(\chi,Z,\varepsilon) = \varepsilon\chi H_1(z) + \varepsilon^3\chi^3 H_3(z) + \cdots.$$

Introducing the inner product

$$\langle f|g\rangle \equiv \int_{-\infty}^{\infty} f\bar{g}\,dx,$$

the linear operator $\mathcal{L}$ is not self-adjoint ($\mathcal{L} \neq \mathcal{L}^\dagger$). In order to solve Eq. (7) we should characterize the kernel of the adjoint of operator $\mathcal{L}$ ($\mathcal{L}^\dagger$). Numerically, we can compute the eigenvalues and eigenfunctions of $\mathcal{L}^\dagger$. Figure 10 shows the spectrum and the eigenfunctions of the critical modes of the $\mathcal{L}^\dagger$. The only element of the kernel of $\mathcal{L}^\dagger$ is $|A_+\rangle$, which is illustrated in Fig. 10 (upper) for a given parameter. Then using this eigenfunction one obtains the following solvability condition to dominate order in ε

$$\dot{P} = \frac{\langle A_+(z)|H_1(z)\rangle}{\langle A_+(z)|\partial_z A_{\text{Ising}}(z)\rangle}\chi.$$

To obtain an equation for the chirality, one can apply the linear operator $\mathcal{L}$ to Eq. (7) and read

$$\varepsilon^2\dot{\chi}\mathcal{L}|A_{as}(z)\rangle = \mathcal{L}^2|W\rangle + \mathcal{L}H(\chi,z,\varepsilon),$$

where by definition $\mathcal{L}|A_{as}(z)\rangle = |\partial_z A_{\text{Ising}}(z)\rangle$ (Jordan base). Thus, one can again apply the solvability condition and obtain

$$\dot{\chi} = \frac{\langle A_+(z)|\mathcal{L}H_1(z)\rangle}{\varepsilon\langle A_+(z)|\partial_z A_{\text{Ising}}(z)\rangle}\chi + \varepsilon\frac{\langle A_+(z)|\mathcal{L}H_3(z)\rangle}{\langle A_+(z)|\partial_z A_{\text{Ising}}(z)\rangle}\chi^3,$$

where the first term on the right is proportional to the bifurcation parameter of the transition, that is, this coefficient is zero at the transition. Scaling

$$\chi = \sqrt{-\varepsilon\frac{\langle A_+(z)|\partial_z A_{\text{Ising}}(z)\rangle}{\langle A_+(z)|\mathcal{L}H_3(z)\rangle}}\chi'$$

and introducing the constant

$$c \equiv \frac{\langle A_+(z)|H_1(z)\rangle}{\langle A_+(z)|\partial_z A_{\text{Ising}}(z)\rangle} * \sqrt{-\varepsilon\frac{\langle A_+(z)|\partial_z A_{\text{Ising}}(z)\rangle}{\langle A_+(z)|\mathcal{L}H_3(z)\rangle}},$$

$$\eta \equiv \frac{\langle A_+(z)|\mathcal{L}H_1(z)\rangle}{\varepsilon\langle A_+(z)|\partial_z A_{\text{Ising}}(z)\rangle}$$

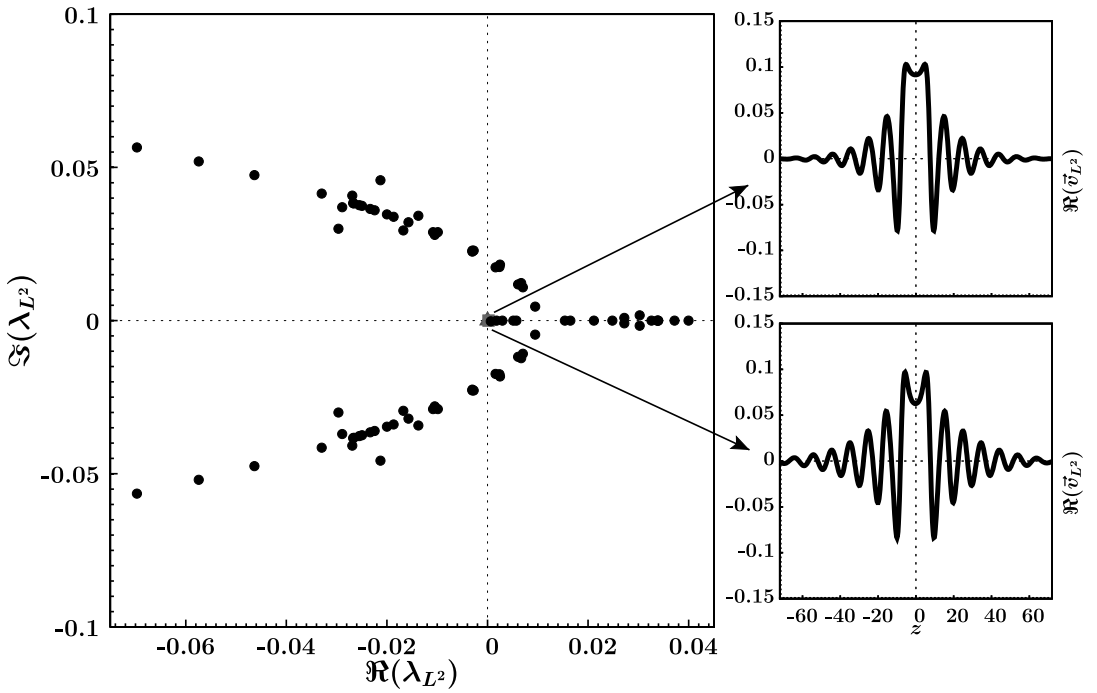

Fig. 9. Spectrum of the square of linear operator ($\mathcal{L}^2$) of the model (5) with $\gamma = 0.6$, $\mu = 0.2$, $\nu = -0.06$, $b = 0.167$, $\delta = 0.225$ and $\alpha = 0.175$. Inset figures are the real part of the eigenfunctions of the respective critical modes.

one obtains the following set of equations for the critical modes

$$\begin{aligned} \dot{P} &= c\chi', \\ \dot{\chi}' &= \eta\chi' - \chi'^3. \end{aligned} \tag{8}$$

The coefficients $\{c, \eta\}$ can be computed numerically for the specific values of the parameters. Hence, wall speed ($\dot{P} \equiv v.$) is proportional to the chirality and the chirality exhibits a stationary pitchfork bifurcation at $\eta = 0$. Subsequently, for negative η, an

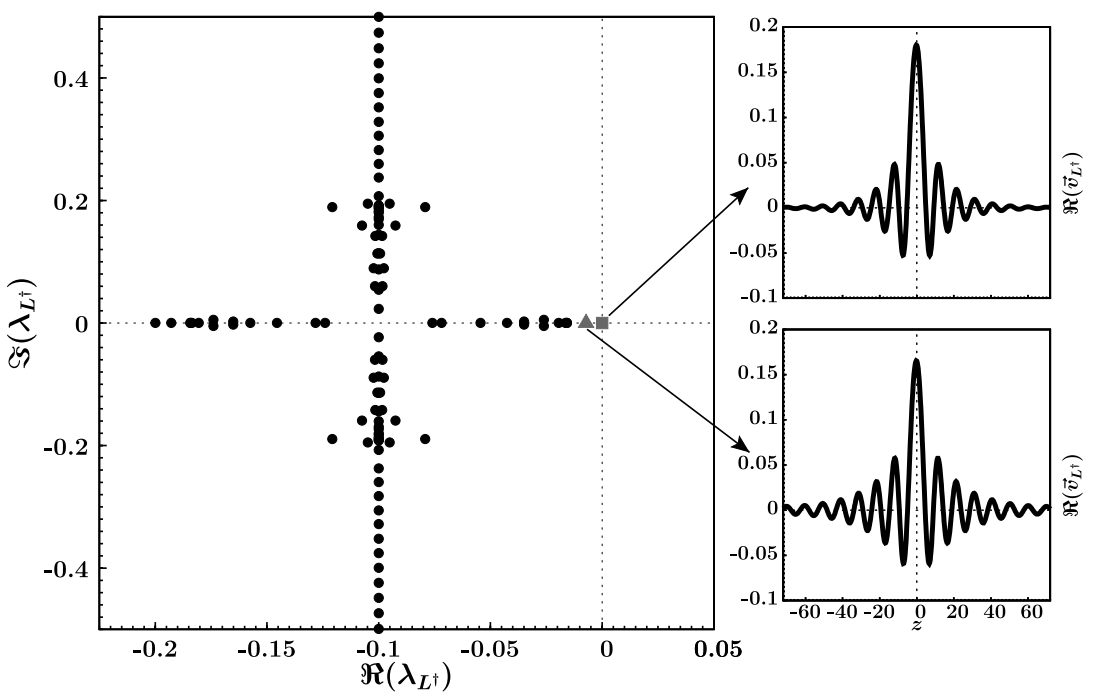

Fig. 10. Spectrum of the operator ($\mathcal{L}^\dagger$) of the model (5) with $\gamma = 0.6$, $\mu = 0.2$, $\nu = -0.06$, $b = 0.167$, $\delta = 0.225$ and $\alpha = 0.175$. Inset figures are the real part of the eigenfunctions of the respective critical modes.

initial asymmetric wall moves some transient and it becomes a motionless interface. On the contrary, for positive η, an initial asymmetric wall moves some transient to become a moving domain wall with well-defined velocity $\dot{P} = v = c\sqrt{\eta}$. Depending on the form of the initial condition the wall propagates to the left or to the right. Using the above equation we can obtain the following equation for speed

$$\dot{v} = \eta v - \frac{v^3}{c^2}. \tag{9}$$

This equation has been obtained in the reaction–diffusion model [Elphick *et al.*, 1995], and nonlinear optics [Michaelis *et al.*, 2001]. However, it is important to note that the nonvariational Ising–Bloch transition is characterized by the two-order parameter $\{P, \chi'\}$. The model (8) describes a stationary bifurcation with two modes and one eigenfunction, which is denoted in the Anorld notation as 0^2 instability [Arnold, 1983]. In the special case of $c = 0$ — there is an stationary bifurcation characterized by two different eigenfunctions — the system exhibits a Ising–Bloch transition, however the Bloch type wall is motionless. This is the classical case observed in magnetic system, where the transition is in equilibrium [Coullet *et al.*, 1990].

5. Conclusions

In the last decades several parametric systems have been studied experimentally and theoretically. The theoretical model most considered is the parametrically driven damped nonlinear Schrödinger equation, however this approach cannot describe the features of the uniform oscillations observed in a parametrically driven magnetic wire and a vertically driven pendula chain. Amending this model with high order terms, one can recover the features of these states. Hence, the stability property of these states is given by high nonlinearities.

The non-null uniform states exhibited by the amended amplitude equation are equivalent states. Then we expect to observe a motionless domain wall between them. However, due to the nonvariational nature of the model (5) and the spontaneous spatial breaking of symmetry this amended model exhibits a nonvariational Ising–Bloch transition. Thus, this system exhibits moving domain walls. Close to this transition, we have derived a simple set of ordinary differential equations for the position and chirality — amplitude of asymmetric modes — of the domain walls, Eq. (8). This set of equations allows us to understand in a simple manner the Ising–Bloch type transition.

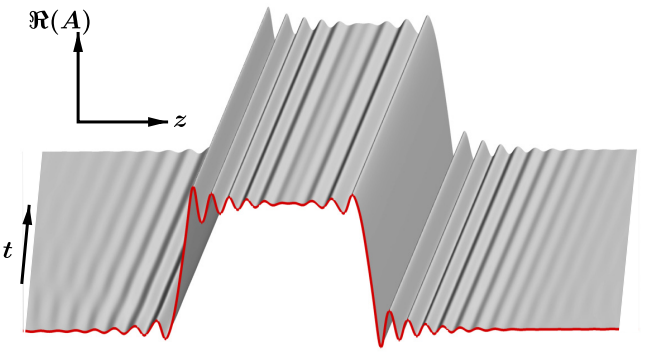

Fig. 11. Spatio-temporal diagram of moving localized domain exhibited by model (5) with $\gamma = 0.8$, $\mu = 0.2$, $\nu = -0.07$, $b = 0.167$, $\delta = 0.3$ and $\alpha = 0.233$.

Parametrically driven systems like magnetic wire forced with a transversal oscillatory magnetic field and vertically driven damped pendula chain close to the strong parametric resonance — systems forced with the double of natural frequency — are described by amended parametrically driven damped nonlinear Schrödinger equation (5). Hence, these systems exhibit a nonvariational Ising–Bloch transition. Moreover, we find a strongly agreement with the numerical simulations.

In addition, Ising wall exhibits a well-defined spatial damping oscillation (cf. Fig. 11). It is well known that the nature of the kink and antikink interactions alternates between attractive and repulsive [Clerc *et al.*, 2005] when the walls have spatial damped oscillation. Therefore, it is expected to find a family of localized states with thickness roughly multiples of the characteristic length of the damped spatial oscillation present in the kink solution. Inside Bloch type solution region these localized domains become moving (cf. Fig. 11). Study and applications of these localized domains are in progress.

Acknowledgments

The simulation software *DimX*, developed at INLN (France), has been used for some numerical simulations presented in this paper. The authors thanks the support of ring program ACT15 of *Programa Bicentenario* of Chilean Government. M. G. Clerc acknowledges the financial support of FONDAP grant 11980002. D. Laroze thanks the partial support of ring program ACT24 of *Programa Bicentenario* of Chilean Government, Millennium Science Nucleus P06-022-F, Convenio de desempeño UTA

MECESUP-2 and Fondecyt 11080229. S. Coulibaly thanks the financial support of Fondecyt 3080041.

References

Arnold, V. I. [1983] *Geometrical Methods in the Theory of Ordinary Differential Equations* (Springer, New York).

Barashenkov, I. V., Bogdan, M. M. & Korobov, V. I. [1991] "Stability diagram of the phase-locked solitons in the parametrically driven, damped nonlinear Schrödinger equation," *Europhys. Lett.* **15**, 113–118.

Barra, F., Descalzi, O. & Tirapegui, E. [1996] "Non variational effects in nonequilibrium systems," *Phys. Lett. A* **221**, 193–196.

Bulaevsky, L. N. & Ginzburg, V. L. [1964] "Temperature dependence of the shape of the domain wall in ferromagnetics and ferroelectrics," *Sov. Phys. JETP* **18**, 530–535.

Burton, W. K., Cabrera, N. & Frank, F. C. [1951] "The growth of crystals and the equilibrium structure of their surfaces," *Phil. Trans. Roy. Soc. London A* **243**, 299–358.

Clerc, M., Coullet, P. & Tirapegui, E. [1999a] "Lorenz bifurcation: Instabilities in quasi-reversible systems," *Phys. Rev. Lett.* **83**, 3820–3823.

Clerc, M., Coullet, P. & Tirapegui, E. [1999b] "The Maxwell–Bloch description of 1/1 resonances," *Opt. Commun.* **167**, 159–164.

Clerc, M., Coullet, P. & Tirapegui, E. [2001] "The stationary instability in quasi-reversible systems and the Lorenz pendulum," *Int. J. Bifurcation and Chaos* **11**, 591–603.

Clerc, M. G., Nagaya, T., Petrossian, A., Residori, S. & Riera, C. [2004] "First-order Fredericksz transition and front propagation in a liquid crystal light valve with feedback," *Eur. Phys. J. D* **28**, 435–445.

Clerc, M. G., Escaff, D. & Kenkre, V. M. [2005] "Patterns and localized structures in population dynamics," *Phys. Rev. E* **72**, 056217.

Clerc, M. G., Coulibaly, S. & Laroze, D. [2008] "Localized state beyond asymptotic perimetrically driven amplitude equation," *Phys. Rev. E* **77**, 056209.

Coullet, P., Lega, J., Houchmanzadeh, B. & Lajzerowicz, J. [1990] "Breaking chirality in nonequilibrium systems," *Phys. Rev. Lett.* **65**, 1352–1355.

Cross, M. & Hohenberg, P. [1993] "Pattern formation outside of equilibrium," *Rev. Mod. Phys.* **65**, 851–1112.

Denardo, B., Galvin, B., Greenfield, A., Larraza, A., Putterman, S. & Wright, W. [1992] "Observation of localized structures in nonlinear lattices: Domain walls and kinks," *Phys. Rev. Lett.* **68**, 1730–1733.

Gilli, J. M., Morabito, M. & Frisch, T. [1994] "Ising–Bloch transition in a nematic liquid crystal," *J. Phys. II* **4**, 314–331.

Graham, R. & Tel, T. [1986] "Nonequilibrium potential for coexisting attractors," *Phys. Rev. A* **33**, 1322–1337.

Goldstein, R. E., Gunaratne, G. H., Gil, l. & Coullet, P. [1991] "Hydrodynamic and interfacial patterns with broken space-time symmetry," *Phys. Rev. A* **43**, 6700–6721.

Haim, D., Li, G., Ouyang, Q., McCormick, W. D., Swinney, H. L., Hagberg, A. & Meron, E. [1996] "Breathing spots in a reaction–diffusion system," *Phys. Rev. Lett.* **77**, 190–193.

Longhi, S. [1996] "Stable multiple pulses in a nonlinear dispersive cavity with parametric gain," *Phys. Rev. E* **53**, 5520–5522.

Michaelis, D., Peschel, U., Lederer, F., Skryabin, D. V. & Firth, W. J. [2001] "Universal criterion and amplitude equation for a nonequilibrium Ising–Bloch transition," *Phys. Rev. E* **63**, 066602.

Murray, J. D. [1989] *Mathematical Biology* (Springer-Verlag, Berlin).

Nicolis, G. & Prigogine, I. [1977] *Self-Organization in Nonequilibrium Systems* (John Wiley and Sons, NY).

Residori, S., Petrossian, A., Nagaya, T., Riera, C. & Clerc, M. G. [2004] "Fronts and localized structures in a liquid-crystal-light-valve with optical feedback," *Physica D* **199**, 149–165.

van Saarloos, W. [2003] "Front propagation into unstable states," *Phys. Rep.* **386**, 29–222.

Zhang, W. & Viñal, J. [1995] "Secondary instabilities and spatiotemporal chaos in parametric surface waves," *Phys. Rev. Lett.* **74**, 690–693.